Biochimica et Biophysica Acta 1808 (2011) 674–683

Contents lists available at ScienceDirect

Biochimica et Biophysica Acta

journal homepage: www.elsevier.com/locate/bbamem

Conformational choreography of a molecular switch region in myelin basic protein—Molecular dynamics shows induced folding and secondary structure type conversion upon threonyl phosphorylation in both aqueous and membrane-associated environments

Eugenia Polverini [a], Eoin P. Coll [b], D. Peter Tieleman [b], George Harauz [c,*]

[a] Dipartimento di Fisica, Università di Parma, V. le Usberti, 7/A, 43100 Parma, Italy
[b] Department of Biological Sciences, University of Calgary, 2500 University Drive NW, Calgary, AB T2N 1N4, Canada
[c] Department of Molecular and Cellular Biology, University of Guelph, 50 Stone Road East, Guelph, ON N1G 2W1, Canada

ARTICLE INFO

Article history:
Received 29 August 2010
Received in revised form 10 November 2010
Accepted 23 November 2010
Available online 3 December 2010

Keywords:
Molecular dynamics
Myelin basic protein
Phosphorylation
PPII structure
Intrinsically disordered protein

ABSTRACT

The 18.5 kDa isoform of myelin basic protein is essential to maintaining the close apposition of myelin membranes in central nervous system myelin, but its intrinsic disorder (conformational dependence on environment), a variety of post-translational modifications, and a diversity of protein ligands (e.g., actin and tubulin) all indicate it to be multifunctional. We have performed molecular dynamics simulations of a conserved central segment of 18.5 kDa myelin basic protein (residues Glu80–Gly103, murine sequence numbering) in aqueous and membrane-associated environments to ascertain the stability of constituent secondary structure elements (α-helix from Glu80–Val91 and extended poly-proline type II from Thr92–Gly103) and the effects of phosphorylation of residues Thr92 and Thr95, individually and together. In aqueous solution, all four forms of the peptide bent in the middle to form a hydrophobic cluster. The phosphorylated variants were stabilized further by electrostatic interactions and formation of β-structures, in agreement with previous spectroscopic data. In simulations performed with the peptide in association with a dimyristoylphosphatidylcholine bilayer, the amphipathic α-helical segment remained stable and membrane-associated, although the degree of penetration was less in the phosphorylated variants, and the tilt of the α-helix with respect to the plane of the membrane also changed significantly with the modifications. The extended segment adjacent to this α-helix represents a putative SH3-ligand and remained exposed to the cytoplasm (and thus accessible to binding partners). The results of these simulations demonstrate how this segment of the protein can act as a molecular switch: an amphipathic α-helical segment of the protein is membrane-associated and presents a subsequent proline-rich segment to the cytoplasm for interaction with other proteins. Phosphorylation of threonyl residues alters the degree of membrane penetration of the α-helix and the accessibility of the proline-rich ligand and can stabilize a β-bend. A bend in this region of 18.5 kDa myelin basic protein suggests that the N- and C-termini of the proteins can interact with different leaflets of the myelin membrane and explain how a single protein can bring them close together.

1. Introduction

One of the major proteins in the central nervous system myelin sheath is myelin basic protein (MBP). In the adult brain, the 18.5 kDa isoform predominates and is essential to myelin stability and homeostasis [1–3]. This protein is structurally polymorphic and multifunctional [4–9]. There is a central, highly-conserved segment (Fig. 1):

$$E^{80}NPVVHFFKNI^{90}VTPRTPPPSQ^{100}GKG^{103}$$

(using murine 18.5 kDa isoform sequence numbering), within which there are two successive structural motifs with different, but perhaps correlated, functionality. First, there is a membrane-associating amphipathic α-helix, demonstrated variously by circular dichroism (CD), electron paramagnetic resonance (EPR), and solution and solid-state nuclear magnetic resonance (NMR) spectroscopy [9–16], comprising residues V83–T92 and representing an immunodominant epitope in multiple sclerosis. Following this segment is a proline-rich segment envisaged by us to be an extended strand that can adopt a

Abbreviations: CD, circular dichroism; DMPC, dimyristoylphosphatidylcholine; EPR, electron paramagnetic resonance; MBP, myelin basic protein; MD, molecular dynamics; NMR, nuclear magnetic resonance; PPII, poly-proline type II conformation; PhT, phosphorylated threonine; RMSD, root mean square deviation

* Corresponding author. Tel.: +1 519 824 4120x52535; fax: +1 519 837 1802.
E-mail address: gharauz@uoguelph.ca (G. Harauz).

0005-2736/$ – see front matter © 2010 Elsevier B.V. All rights reserved.
doi:10.1016/j.bbamem.2010.11.030

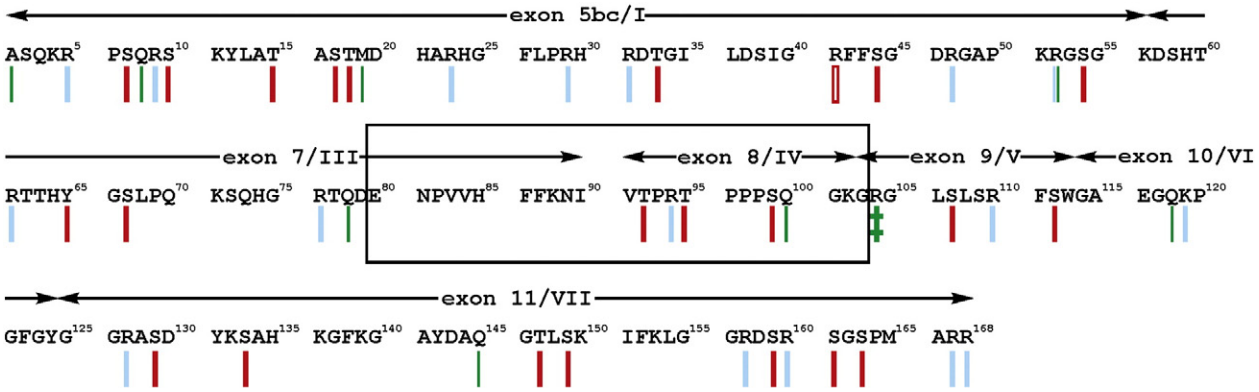

Fig. 1. Amino acid sequence of 18.5 kDa murine MBP. The exons are also indicated—Arabic/Sanskrit numbering with reference to the full gene of oligodendrocyte lineage and Roman numerals indicating the "classic" gene. The peptide fragment simulated here is denoted EPPH and is indicated by a box; it comprises the latter part of exon 7 and all of exon 8 and is highly-conserved in sequence. The molecular barcode due to diverse and combinatorial post-translational modifications is as follows: red bar, phosphorylation (S, T, Y); hollow red bar, an unusual case of arginyl phosphorylation at R41; ice blue bar, citrullination; green bar, diverse PTMs (acylation, deamidation, ADP-ribosylation, sulphoxide oxidation of methionine); crossed green bar, methylation (either ω-$N^{G'}$-mono-methylation or symmetric ω-N^{G},N'^{G}-di-methylation of R104). The murine residues T92 and T95 are MAP kinase phosphorylation sites, lying in the vicinity of a putative molecular switch. This figure was adapted with permission from reference [7].

poly-proline type II (PPII) conformation, as demonstrated by CD spectroscopy [8,17]. Since MBP has been demonstrated to bind SH3-domain-containing proteins [17,18], for which the canonical core ligand is XP–x–XP in a left-handed PPII structure, we consider the MBP segment T92–P97 to represent most of the SH3-target, although the full details of binding have not yet been elucidated.

Our current working model of this region of the protein is that the amphipathic α-helix would associate with the membrane and would position the SH3-target and proline repeat $TP^{93}RTP^{96}PPS$ outside the membrane into the cytoplasmic milieu (Fig. 2). Residues Phe86 and Phe87 should anchor the helix into the membrane interior. We consider this central region of 18.5 kDa MBP to constitute a "molecular switch" because of the number and variety of post-translational modifications that may represent different levels of control, particularly phosphorylation of residues T92 and T95 by mitogen-activated protein kinases (reviewed in [4–8]). In general, MBP is a conformationally dynamic protein for which it is difficult to define an experimentally tractable system to probe structure at the amino acid level by NMR spectroscopy, say [6–9,19,20]. For this reason, we use molecular dynamics (MD) simulations here to study at atomic detail the structure that this segment of the protein adopts in aqueous solution and in a phospholipid bilayer, its association with the membrane, and the effects of threonyl phosphorylation. The results demonstrate both secondary and tertiary structural changes induced by environment and modifications, some of which explain previous experimental findings and all of which represent hypotheses for future spectroscopic evaluation.

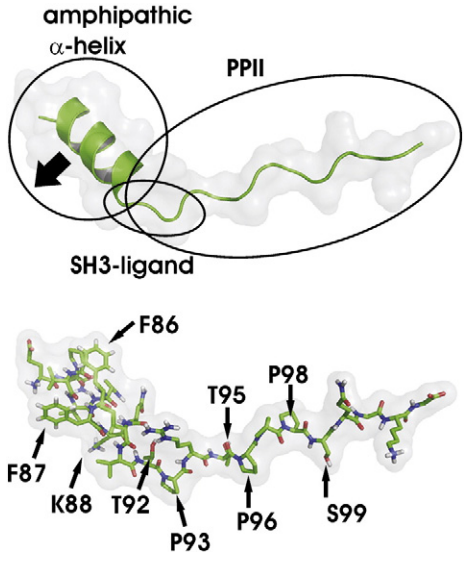

Fig. 2. Starting conformation of EPPH model, showing secondary structure elements and various residues, including the MAP kinase phosphorylation sites at Thr92 and Thr95.

2. Methods

A starting molecular model of the segment

$$NH_3^+ - E^{80}NPVVHFFKNI^{90}VTPRTPPPSQ^{100}GKG^{103} - COO^-$$

was constructed using SYBYL software version 7.0 (SYBYL, Tripos Associates Inc., St. Louis, MO). Based on results arising from diverse experimental data as described above [8,12,17,21,22] and slightly extending the putative structured regions, the starting model comprised an amphipathic α-helix from residue E^{80} to residue V^{91} and an extended strand in a left-handed poly-proline type II (PPII) conformation from residue T^{92} to residue G^{103} (Fig. 2).

All proline residues were in *trans* configuration [23,24], and the histidyl residues were left unprotonated (neutral), in accordance with experimental pH values in the literature [8,12,17,21,22]. Using SYBYL software, a phosphate group (in the −2 charge state) was added onto residues T92 (PhT92) and T95 (PhT95), building three additional phosphorylated peptides: two with a single phosphorylated residue (PhT92 or PhT95) and one with phosphorylation of both threonines, for comparison with the unmodified peptide.

Molecular dynamics simulations were performed using the GROMACS 4.0.5 software package [25] and the Gromos96 ffG53a6 force field [26]. Molecular dynamics runs were performed using 64 processors at Compute Canada/SHARCNET facilities (https://www.sharcnet.ca). All four peptides (unmodified, PhT92, PhT95, and PhT92–PhT95) were simulated in two different environments. The first was in aqueous solution, building a box with a minimum of a 1 nm layer of water around the peptide and adding salt and counter-ions (sodium and chloride) to the system to obtain an overall zero charge and to reach a physiological salt concentration of 0.15 M. The second was in association with a lipid bilayer of dimyristoylphosphatidylcholine (DMPC), using publicly accessible DMPC structural coordinates (http://moose.bio.ucalgary.ca/index.php?page=Structures_and_Topologies). The DMPC bilayer was pre-equilibrated for

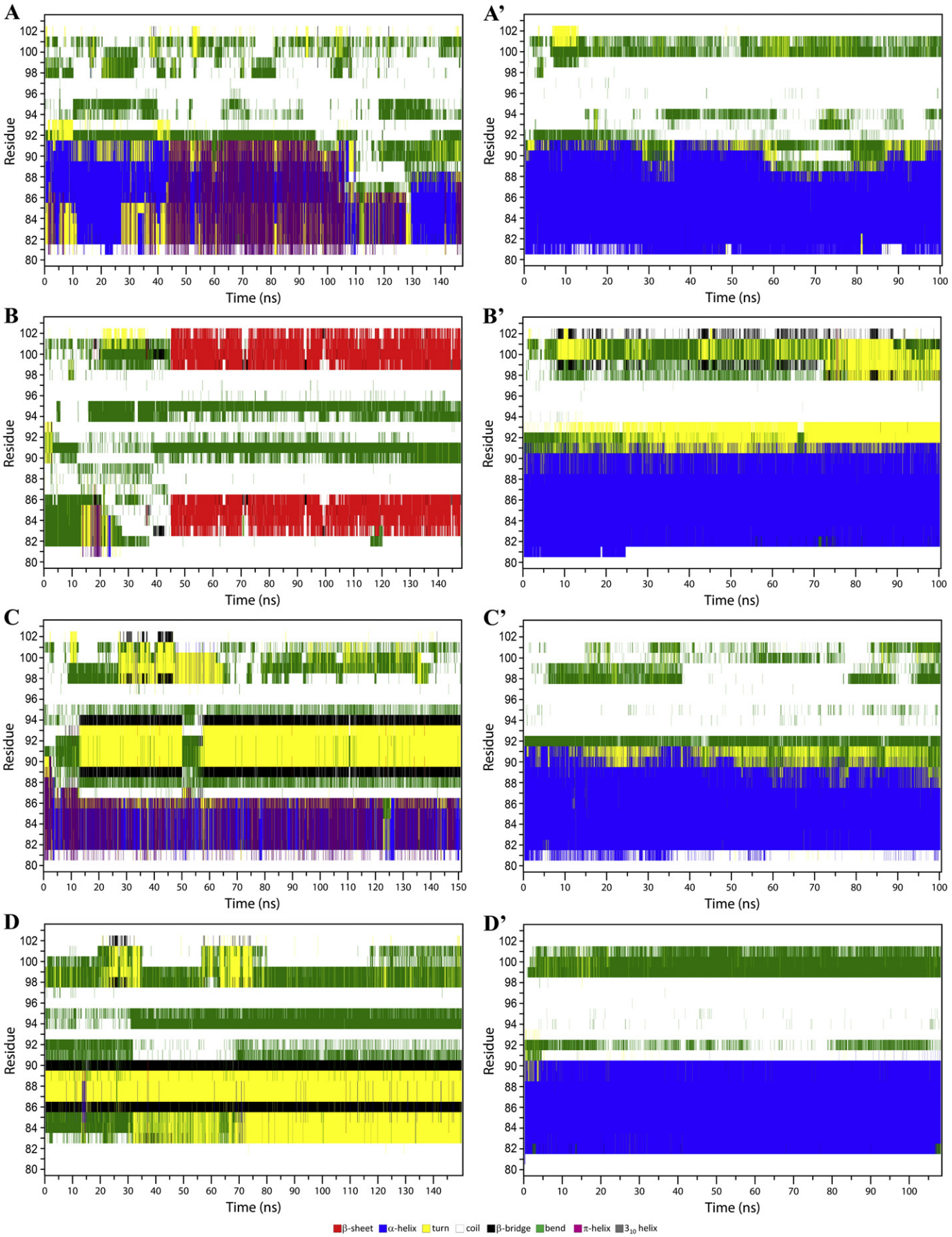
A
A'
B
B'
C
C'
D
D'
Residue
Time (ns)
β-sheet
α-helix
turn
coil
β-bridge
bend
π-helix
3₁₀ helix

20 ns. To construct the simulation box, each peptide was first positioned at the surface of the DMPC bilayer, and the six lipid molecules present in a radius of 1 Å around the peptide were manually deleted. The system was solvated with a layer of water molecules about 3 nm thick at each side of the membrane and counter-ions were added as above.

After a minimization of the whole system in water, a classical position restrained MD of 50 ps was run keeping the peptide position fixed, whereas in the DMPC system, two position restrained MDs were performed: the first keeping both the peptide and the DMPC bilayer fixed (100 ps), the second keeping only the peptide fixed (1 ns). Periodic boundary conditions were applied in both environments. The full MD simulations were run for 160 ns in water and 100 ns in membrane, at 300 K and 1 atm, with a time step of 2 fs. Temperature coupling was made using velocity rescaling with a stochastic term [27], with a time constant of 0.1 ps. The "protein" and "water + ions" groups were coupled separately to the temperature bath in the aqueous environment, whereas the "protein + DMPC" and "water + ions" groups were coupled separately in the membrane simulations. Pressure coupling was isotropic in aqueous solvent and semi-isotropic in membrane simulations. The Berendsen barostat [28] was used, with a coupling constant of 1 ps.

All the simulations present here were repeated twice, and the results agreed closely. Only one representative simulation is presented here, for simplicity. For visualization and analysis of structural files and trajectories computed by GROMACS, the GROMACS subroutines and the Visual Molecular Dynamics (VMD) program [29] were utilized. The protein contact maps were drawn by means of the WebMol program (available online at http://www.cmpharm.ucsf.edu/cgi-bin/webmol.pl) [30].

3. Results and discussion

3.1. Rationale for starting structure for MD simulations

The starting model for the EPPH peptide represents an approximation of the structure that this protein segment should assume in a membrane environment, as discussed in the Introduction (Fig. 2). The MD simulations performed here were intended to investigate the overall structural propensity and stability of the peptide in aqueous and membrane-associated environments. Since MBP is a dynamic protein even when membrane-associated, the idea of a defined, rigid conformation does not apply [9,20]. Moreover, even the precise disposition of the membrane-anchoring amphipathic α-helical motif (extent of helicity, tilt with respect to the membrane) depends on the extent of protein post-translational modifications [14] and on membrane lipid composition [12,16]. Here, a short control simulation in aqueous solution was initially run on a peptide with protected N- and C-termini (results not shown). We concluded that the zwitterionic form of the peptide did not seem to influence the dynamics significantly because the presence of an oppositely charged residue at both N- and C-termini partially shielded the net charges at the termini. Several MD simulations of shorter peptide fragments of MBP in aqueous solution and organic solvents have been published in studies of their potential efficacy as agonists or antagonists against multiple sclerosis (e.g., [31]). Our study here differs in that it examines different structural questions on a larger fragment in a membrane environment.

3.2. Peptides in aqueous solution

All MD simulations in the water box were performed for 160 ns each. The results are portrayed in terms of secondary structure (Fig. 3A–D), residue contacts (Fig. 4), and final conformations (Fig. 5). In water, such short protein fragments are usually very flexible and unordered; in addition, an amphipathic α-helical structure is evidently not a stable structure in water, if alone. Therefore, in many cases, the root mean square deviation (RMSD) plots of their trajectories cannot reach a plateau (see Figure S1) due to the presence of many interconverting metastable structures. However, the presence of local transient secondary structures could indicate a structural propensity for some regions of the peptide (cf., [8,9,32]). Here, as could be expected, at the end of the simulation at 160 ns, all peptides reach a quite stable conformation (Fig. 5) that optimizes the exclusion from the solvent of the hydrophobic residues (in particular, the highly hydrophobic F86–F87 residues and the tri-proline (P96–P97–P98) cluster). To achieve this arrangement, both the unmodified and the phosphorylated peptides show a central bend of the backbone, helped in this regard by the P93 residue. The Pro-rich segment keeps a core PPII structure within the P96–P97–P98 cluster.

The unmodified peptide is the more oscillating one (Figure S1 in Supporting Material). Its trajectory shows a flexible but stable helix in the N-terminal part of the epitope segment that swings repeatedly from α- to π-helix and finally closes its hydrophobic surface to the P96–P97–P98 hydrophobic cluster. In this case, the stability of the amphipathic α-helix could be achieved due to the interaction of its hydrophobic surface with the hydrophobic residues of the Pro-rich region.

The phosphorylated peptides reach a quite stable conformation more rapidly (Figure S1). They show different amounts of β-structure, in interesting qualitative agreement with previous experimental CD studies performed on the whole protein [33–36]. The β-contacts, particularly evident in Fig. 4 as the diagonal from the bottom-right to the upper-left corner, are favored by the phosphate groups that interact with basic residues R94 and K88 in a salt bridge manner. In particular, the PhT92 peptide forms a β-hairpin structure that is very stable also for the optimization of the hydrophobic interactions. Due to the different position of the phosphate group, the β-bridge in the PhT95 peptide is shorter and limited to the central region of the backbone. In the double-phosphorylated peptide, probably due to the high amount of net charged residues in such a short sequence (6 negative and 4 positive ones—including the 2 termini—that gives a net charge of −2, exactly the opposite of the unmodified peptide), the structure compacts very early into a globule, with the electrostatic interacting residues that strengthen a hydrophobic core.

For the PhT95 phosphorylated peptide only, a significant amount of helical structure is preserved in the epitope segment, whereas the T92 phosphorylation seems to create interactions that tend to disrupt the helical structure favoring a very stable β-hairpin.

3.3. Peptides in association with DMPC bilayer

The starting orientation of the peptide with respect to the membrane bilayer was chosen in agreement with experimental data to date (cited in the Introduction), various functional and experimental hypotheses, and with electrostatic/hydrophobic characteristics: the amphipathic α-helix was inserted at the membrane surface,

Fig. 3. Secondary structure of EPPH models over the course of the MD simulations in solution (capital letters without the prime) and in a DMPC bilayer (capital letters with the prime). (A and A') EPPH-unmodified; (B and B') EPPH–PhT92; (C and C') EPPH–PhT95; (D and D') EPPH–PhT92–PhT95. Color code: red, β-sheet; blue, α-helix; yellow, turn; white, coil; black, β-bridge; green, bend; purple, π-helix; gray, 3_{10}-helix.

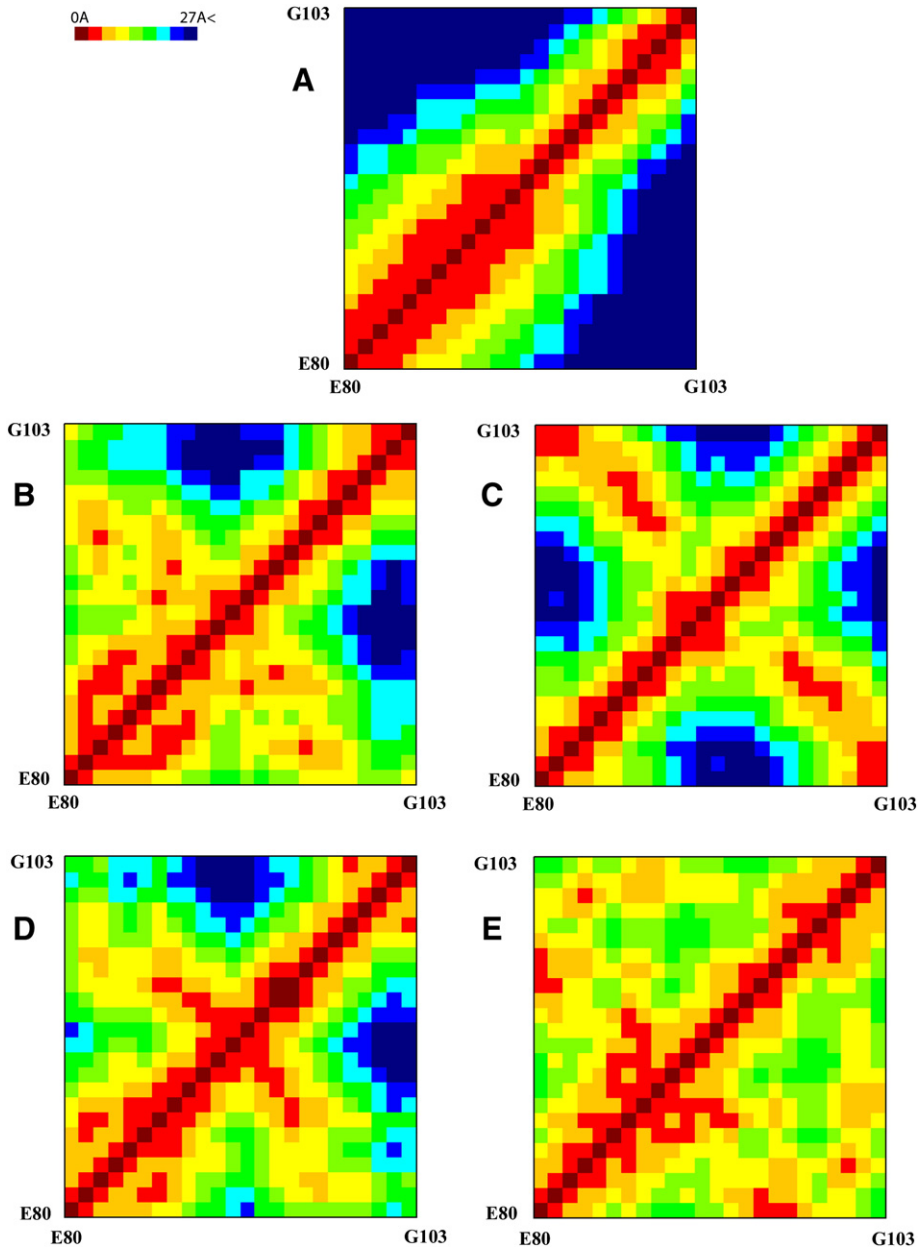

Fig. 4. Contact maps showing proximity of residues within EPPH in the (A) starting model, and after a 160 ns MD simulation in aqueous solution of (B) EPPH-unmodified; (C) EPPH–PhT92; (D) EPPH–PhT95; (E) EPPH–PhT92–PhT95. The squares indicating the residue–residue distance are colored from dark red (0 Å distance) to dark blue (>27 Å distance). The large band along the main diagonal from the bottom-left to the upper-right corner shows the local contacts such as helical structures. The diagonal from the bottom-right to the upper-left corner shows the amount of β-contacts.

with the two Phe residues (F86 and F87) pointing down towards the hydrophobic tails and the charged/polar residues pointing towards the polar head groups or the solvent; the PPII structure was oriented outwards with respect to the membrane, in the aqueous solvent (Fig. 6).

We used the DMPC phospholipids as a model membrane system with neutral net charge to first investigate the interaction with a membrane of these peptides. The 18.5 kDa MBP has, in fact, been demonstrated to penetrate deeply into this kind of lipid [37]. It is known that electrostatic interaction is the force that drives this basic protein towards the negatively-charged polar groups of the myelin membrane [37,38], and simulations with negatively-charged lipids will be the subject of a future study. Here, to overcome partially the electrostatic driving force problem, we positioned the peptide already at the surface of the lipid bilayer.

All peptide-DMPC membrane MD simulations were performed for 100 ns each. The results are portrayed in terms of secondary structure (Fig. 3A'–D') and final conformations (Fig. 7). In DMPC, the α-helix of the epitope segment is very stable for all four peptides (Fig. 3A'–D'), as we can also see from the RMSD plot (Figure S2), and penetrates deeper into the membrane as the simulation proceeds (Fig. 7). The PPII region remains quite extended and oscillating (Figure S2) but with the P96–P97–P98 cluster in a very stable PPII conformation.

The membrane penetration is especially strong in the unmodified peptide, in which the two bulky and highly hydrophobic F86 and F87 residues drag the hydrophobic region linking the Pro-rich segment (in particular, residues I90 and V91, but also P93) down into the membrane (Fig. 7A). The polar N- and C-termini, and the basic residues of the polar α-helix surface, interact with the polar head groups of the phospholipids. The α-helix, therefore, tilts its axis, in

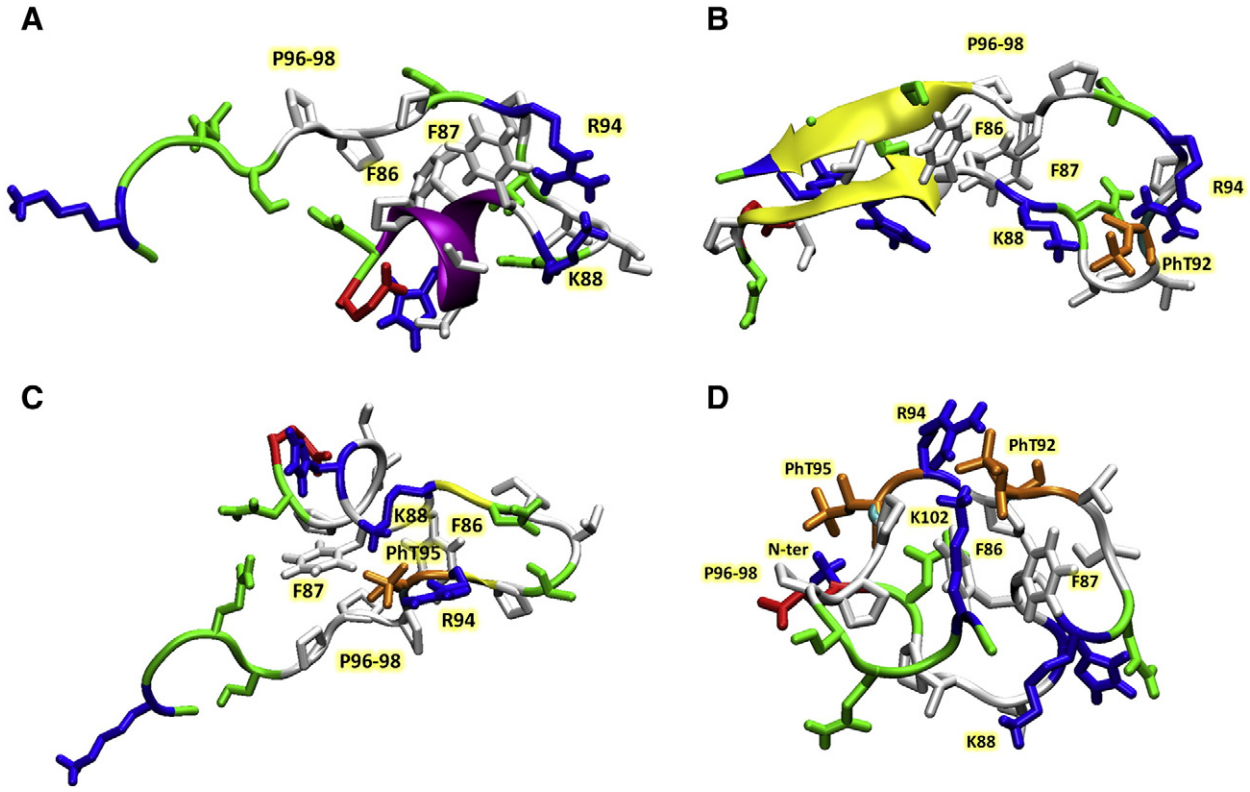

Fig. 5. Final (160 ns) structures of EPPH peptides in solution. (A) EPPH-unmodified; (B) EPPH–PhT92; (C) EPPH–PhT95; (D) EPPH–PhT92–PhT95. Residues are colored by type (green, polar; white, hydrophobic; blue, basic; red, acidic; orange, phosphorylated). The ordered secondary structure is highlighted in cartoon (purple, helix; yellow, β-sheet and β-bridge).

strong agreement with what was previously suggested on the basis of EPR and NMR spectroscopic data [8,12–14,16]. In these earlier studies, based on the depth of penetration of the different residues into the lipid bilayer, a tilt was proposed with respect to the plane of the bilayer in which the N-terminus–C-terminus axis of the helical segment has a downward direction into the membrane. In Fig. 8, the tilt angle of the helix axis is shown as a function of time for the four peptides. The tilt angle here is plotted as the angle of the helix axis vectors (N-terminus–C-terminus direction) with respect to a plane parallel to the membrane surface; the positive values indicate a C-terminus above the horizontal plane, and the negative ones, below. The unmodified peptide shows a pattern clearly different from the other phosphorylated peptides, with a decreasing tilt angle that reflects the insertion of the C-terminus into the membrane while leaving the N-terminus at the surface.

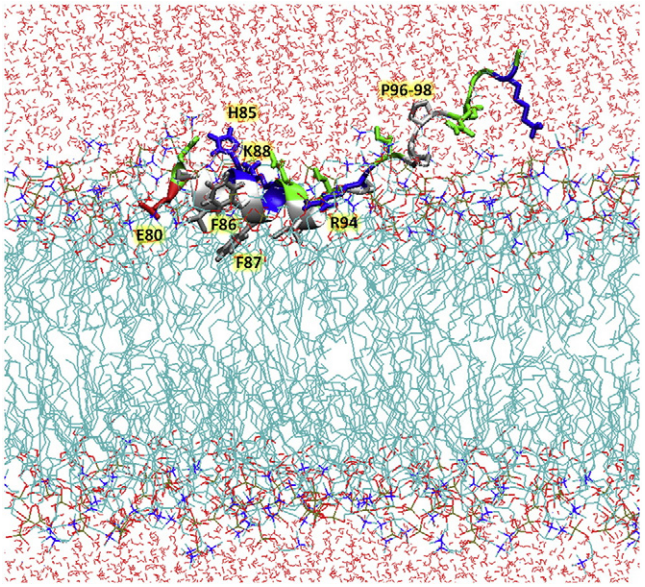

Fig. 6. Starting configuration of EPPH model positioned over a DMPC bilayer. The color code is as in Fig. 5, except for the color of the ordered secondary structure that is also by residue type. In this way, the hydrophobic surface of the amphipathic α-helix is clearly visible in white, whereas the polar surface is in color.

In contrast, the patterns of the three phosphorylated peptides are similar to each other but opposite from the unmodified one. In fact, the threonine phosphate group interacts with the lipid polar head groups and with the solvent counter-ions, maintaining the Pro-rich region more solvent-exposed and the stable α-helix less deeply inserted (Figs. 7B–D). For the mono-phosphorylated fragments, the helix axis stays roughly horizontal with respect to the membrane (Figs. 7B, C, and 8), whereas in the double-phosphorylated variant, the two phosphates pull up the peptide and the helix tilts in the opposite direction (Figs. 7D and 8), with its C-terminus at the surface of the membrane and the N-terminus more deeply inserted.

3.4. Summary of structural propensity of peptide conformations

The MD simulations described here show that the immunodominant epitope of MBP already has an α-helical propensity in water and forms a stable amphipathic α-helical structure in association with the membrane, in agreement with many previous spectroscopic studies [9,12–14,16,32]. The phosphorylation of threonyl residues has significant effects on the conformation of the protein, as shown here by MD simulations. In water, phosphorylation tends to cause the protein to form β-bridges favored by the interaction between phosphate and basic residues, in agreement with previous experimental data [34–36]. Such a phenomenon may be representative of

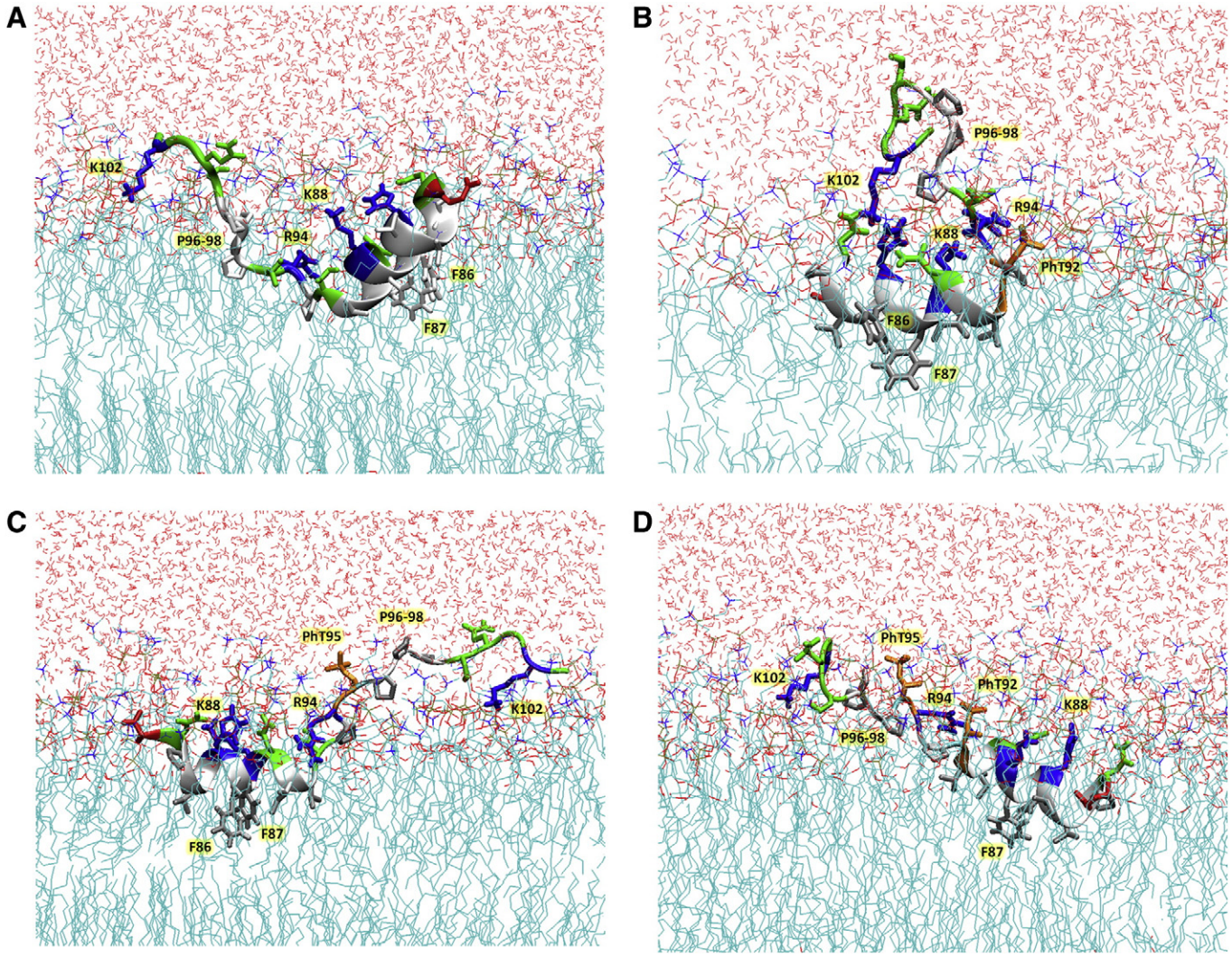

Fig. 7. Final (100 ns) structures of EPPH models interacting with DMPC bilayers. (A) EPPH-unmodified; (B) EPPH–PhT92; (C) EPPH–PhT95; (D) EPPH–PhT92–PhT95. The color code is as in Fig. 6.

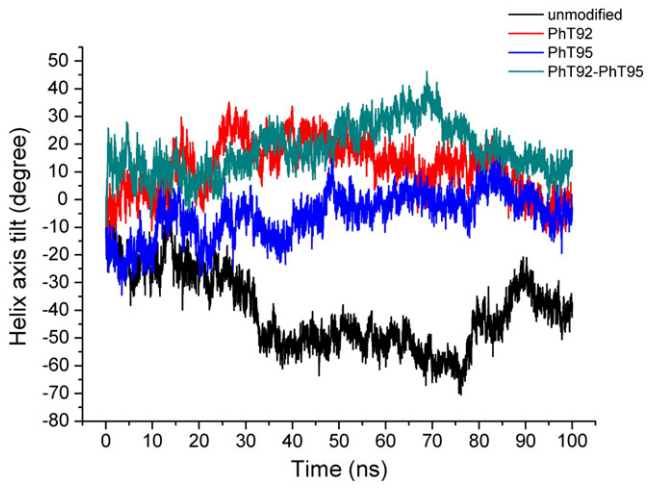

Fig. 8. Helix axis tilt with respect to a plane parallel to the membrane surface as a function of time, for the unmodified (black line), PhT92 (red line), PhT95 (blue line), and PhT92–PhT95 (dark green line) peptides in DMPC. Positive values indicate that the axis vector (N-terminus–C-terminus direction) points upwards over the horizontal plane, and negative values, downwards under the horizontal plane. For axis calculation, residues 2–11 were chosen.

"moonlighting" in which the same segment of a protein can assume different conformations for different tasks [39]. In association with a DMPC membrane, the protein fragment seems to maintain the Pro-rich region—with its PPII core conformation—more solvent-exposed, ready to interact with signaling proteins on the oligodendrocyte membrane. We note that the real cytoplasmic leaflet of the oligodendrocyte membrane in myelin comprises also negatively-charged phospholipids and cholesterol [40], and the interaction of this peptide with more complex membranes will be explored in future studies. The results here are nonetheless of value in interpreting various experimental data.

3.5. Significance—conformational changes and a molecular switch in MBP

The 18.5 kDa isoform of myelin basic protein predominates in adult brain. It is an intrinsically disordered (or better described as conformationally adaptable) protein that gains ordered secondary structure only on association with some binding partner. The protein's three-dimensional conformation within myelin is not known nor how it holds two apposing leaflets of membrane close together. We first address the issue of ordered secondary structure.

In all associations that we have so far investigated structurally by experimental methods (phospholipid membrane, Ca^{2+}-calmodulin,

actin, SH3-domains), the 18.5 kDa MBP isoform has demonstrated a partial induced disorder to order transition, including several α-helical molecular recognition fragments (MoRFs) ([7,8,17,18,21]; cf., [41]). We have spectroscopic evidence that a proline-rich segment potentially forms a left-handed poly-proline type II (PPII) structure that may represent the primary SH3-ligand [8,17]. We have posited that the central, highly-conserved segment (comprising an amphipathic, membrane surface-associated α-helix followed by a PPII structure) may represent a molecular switch (Figs. 1, 2) [8]. This region comprises two mitogen-activated (MAP) kinase sites that are modified during propagation of an action potential [42] and which are correlated with structurally stable myelin [35], albeit less strongly-compacted [33], and with microdomain ("lipid raft") association [43–45]. Phosphorylation at T95 appears to be required for MBP to interact with the WW domain of the prolyl isomerases human Pin1 and yeast ESS1 [46]. There may thus be several kinds of conformational disorder to order transitions occurring in this region, modulated by degree of membrane association and site-specific threonine phosphorylation. In other proteins, phosphorylation affects the stability of α-helices depending on its position inside the helix, tending towards stabilization at the N-terminus and destabilization at the C-terminus [47], and hyperphosphorylation of the microtubule-associated protein tau has been shown to induce PPII structures [48].

Here, the MD simulations in aqueous solution show that threonyl phosphorylation has a potentially large effect on local conformation. Although the PPII core of the P96–P97–P98 region of the peptide remained relatively stable, the peptide bent in the center and the amphipathic α-helical immunodominant epitope appeared to convert to a β-strand. The existence of a β-sheet backbone of MBP had been postulated in early structural models before it was realized that the protein is intrinsically disordered [49–54], and β-sheet has been detected in the intact protein fragments by CD spectroscopy, for example [55], but has not yet been identified at the residue level. Other CD spectroscopic studies of MBP and fragments thereof have indicated an increase in the proportion of β-structure (both sheet and turn) after phosphorylation [34–36,56]. Our MD simulations here show how the formation and stabilization of local β-structure can occur and agree well with these early experimental data.

When the peptide fragment is associated with a lipid bilayer via its amphipathic α-helical membrane-anchoring motif, however, the extended proline-rich segment remains exposed to the aqueous milieu. A good analogy from the literature is that of the microtubule-associated protein MAP2C, in which a different proline-rich motif is kept rigid and extended (in PPII conformation) to enable contacts with other target proteins [57]. The overall configuration of this segment with respect to the membrane supports our contention that it is a significant switch region.

3.6. Isomerization of prolyl residues

Regarding structure and protein–protein interactions, the potential isomerization of prolyl residues in MBP in vivo has been mentioned as a possible signaling or functional control mechanism [7,8,17,55]. Fraser and Deber [23] have investigated the question of proline isomerization in the P96–P97–P98 region of MBP with respect to the hypothesis that *cis* isomers would allow the protein to bend here (see also Nygaard et al. [58]). They found that the spontaneous rate of proline isomerization is very slow and almost negligible and increased to only about 5% in membrane-associated MBP, enabling them to discount the idea of a bend at the tri-proline repeat [23]. Here, we found no evidence for *trans* to *cis* proline isomerization in any of our simulated peptides, which would not be expected in any event on the time scale of these simulations. If it were to occur, such an effect would have a significant change on the protein backbone [22]. We did, however, see a phosphorylation-induced bend in the vicinity of P93 instead of at P96–P97–P98. Thus, it remains plausible that MBP does, indeed, bend in the middle—simply not at the residues first expected and not as a result of proline isomerization. By analogy with other peptides, phosphorylation of the threonyl residues within the TP–R–TP motif has the potential to stabilize the PPII conformation and thus slow the rate of spontaneous isomerization [59].

Given that the immunodominant epitope of the protein is a membrane-associated α-helix, it has been suggested that phosphorylation of these threonyl residues may concomitantly result in a localized *de*stabilization of the preceding α-helix [47] and/or disruption of the C-terminus of the central amphipathic α-helix from the phospholipid membrane, a phenomenon similar to what has been observed for the deiminated protein [14]. Here, however, this segment of the DMPC bilayer-associated peptides remained stably α-helical and phosphorylation served primarily to move the C-terminus out of the membrane. This was not a structural destabilization *per se* but rather served to move the PPII structure out further into the aqueous milieu. Real myelin membranes comprise a mixture of lipids, including negatively-charged ones (as in our experimental systems for EPR and solid-state NMR spectroscopy [12,14,16,20]). Thus, this effect may be even more pronounced in such systems due to the electrostatic repulsion between phosphates and polar head groups, which should enhance the exposure of the phosphorylated peptides at the membrane surface.

3.7. Significance—potential higher-order conformation of 18.5 kDa MBP

The MD simulations presented here showed the potential for tertiary interactions. Although intrinsically disordered proteins generally lack a compact tertiary fold, they can still exhibit higher-order interactions [60]. The microtubule-assembling protein tau has been shown, by FRET (fluorescence resonance energy transfer) and NMR spectroscopy, to exhibit a "double-hairpin" or "paperclip" arrangement in solution [61–64]. Other examples are clusterin, a glycoprotein that binds with high-affinity to various lipids and proteins [65], calpastatin, an inhibitor of the protease calpain [57], and the aforementioned MAP2C [*ibid.*]. Both clusterin and MBP have regions alternately predicted to be ordered and disordered, with regions of high α-helix amphipathicity [8]. The hydrophobic probe ANS (1-anilino-8-naphthalene sulfonate) is bound similarly by clusterin and MBP, with apparent dissociation constants of 70 μM (clusterin [65]) or 30 μM (MBP [66]). These values are similar to those for molten globule proteins and would be 100-times *less* for a rigid structured protein. The term "molten globules" is used to refer to partially-folded protein intermediates, characterized by a compact structure, pronounced secondary structure content, and a lack of a rigidly packed interior. Due to the presence of loosely packed hydrophobic cores, proteins in the molten globule state have a much stronger affinity for ANS-like probes compared with the globule or the fully unfolded states [67,68]. This term is not directly applicable to 18.5 kDa MBP except to convey the idea that this protein may have a loose tertiary arrangement beyond just an extended coil, even in unliganded form.

Fluorescence studies of MBP show intra-molecular quenching of the single tryptophan residue by a quaternary ammonium group of Lys or Arg, as demonstrated by us and by others before that [69–71] (see also [72]). Our studies with hexahistidine-tag-lacking UT-rmC1 and UT-rmC8 variants that we have constructed show that Zn^{2+} cations both stabilize ordered secondary structure [73] and result in the formation of a more compact structure by nanopore analysis [74]. In EPR studies of membrane-associated 18.5 kDa MBP, the overall accessibility of hydrophobic and hydrophilic paramagnetic agents (NiEDDA and O_2) indicates that the bilayers are in closer apposition at the termini of the protein than in the center, which comprises the segment modeled here [75]. These results can be explained by a bend in the protein at this region, which would push the bilayers apart. All in all, there are considerable data to support the hypothesis that MBP

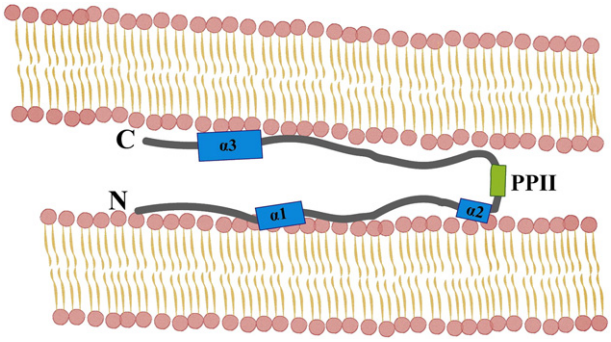

Fig. 9. Schematic representation of 18.5 kDa murine MBP with its N- and C-terminal segments mediating close apposition of two phospholipid bilayers in the simplest model possible, i.e., a hairpin. We present three segments with the potential to form amphipathic α-helices that would interact with the membrane [7,32]: (T33–D46 or α1), (V83–T92 or α2—primary immunodominant epitope), and (A141–L154 or α3—secondary immunodominant epitope and part of the primary calmodulin binding segment). Both the α2 and α3 segments have been experimentally confirmed to form membrane surface-associated α-helices [12,16,75]. Segment P93–Q100 comprises a bend and a poly-proline type II structure. This figure was adapted from reference [75].

has a higher-order topology in both free and membrane-associated form, and the MD simulations performed here suggest that the center of the protein can be a bend point, especially in phosphorylated variants. In this way, two halves of the protein could associate with different myelin membrane leaflets and hold them together as a monomer [16,75,76]. A schematic picture of how the full-length 18.5 kDa MBP could interact with the myelin membrane is depicted in Fig. 9.

4. Conclusions

We have performed MD simulations of a highly-conserved segment of 18.5 kDa MBP in environments that the protein would encounter in either experimental in vitro or physiological in vivo situations. These studies enabled a systematic comparison of induced disorder to order transitions and the structural effects of threonyl phosphorylation whose biological importance remains to be determined. The results confirmed our working model of an amphipathic α-helix whose structure is stabilized by being membrane-bound and whose placement on the membrane orients a flanking proline-rich segment into the cytoplasm where it is accessible to other proteins such as SH3-domain-containing ones. Threonyl phosphorylation causes the α-helix to be less firmly attached to the lipid bilayer. In aqueous solution, these post-translational modifications induce the formation of β-structures that have previously been detected spectroscopically and that stabilize a bend in the protein in this region. The existence of such a bend in the protein supports a model of the myelin sheath in which a single MBP can bring two apposing leaflets of the oligodendrocyte membrane close to each other.

Acknowledgments

These investigations were made possible by the facilities of the Shared Hierarchical Academic Research Computing Network (SHARCNET: www.sharcnet.ca) and Compute/Calcul Canada. This work supported by the Natural Sciences and Engineering Research Council of Canada (GH) and the Canadian Institutes of Health Research (DPT). DPT and GH are grateful to the Alberta Heritage Foundation for Medical Research (AHFMR) for a Visiting Professorship Award. DPT is an AHFMR Scientist.

Appendix A. Supplementary data

Supplementary data to this article can be found online at doi:10.1016/j.bbamem.2010.11.030.

References

[1] A. Privat, C. Jacque, J.M. Bourre, P. Dupouey, N. Baumann, Absence of the major dense line in myelin of the mutant mouse "shiverer", Neurosci. Lett. 12 (1979) 107–112.
[2] C. Readhead, N. Takasashi, H.D. Shine, R. Saavedra, R. Sidman, L. Hood, Role of myelin basic protein in the formation of central nervous system myelin, Ann. NY Acad. Sci. 605 (1990) 280–285.
[3] MoscarelloM.A. , Myelin basic protein, the "executive" molecule of the myelin membrane, in: JuurlinkB.H.J. , DevonR.M. , DoucetteJ.R. , NazaraliA.J. , SchreyerD.J. , VergeV.M.K. (Eds.), Cell Biology and Pathology of Myelin: Evolving Biological Concepts and Therapeutic Approaches, Plenum Press, New York, 1997, pp. 13–25.
[4] J.M. Boggs, Myelin basic protein: a multifunctional protein, Cell. Mol. Life Sci. 63 (2006) 1945–1961.
[5] J.M. Boggs, Myelin Basic Protein, Nova Science Publishers, Hauppauge, NY, 2008.
[6] G. Harauz, N. Ishiyama, C.M.D. Hill, I.R. Bates, D.S. Libich, C. Farès, Myelin basic protein—diverse conformational states of an intrinsically unstructured protein and its roles in myelin assembly and multiple sclerosis, Micron 35 (2004) 503–542.
[7] G. Harauz, V. Ladizhansky, J.M. Boggs, Structural polymorphism and multifunctionality of myelin basic protein, Biochemistry 48 (2009) 8094–8104.
[8] G. Harauz, D.S. Libich, The classic basic protein of myelin—conserved structural motifs and the dynamic molecular barcode involved in membrane adhesion and protein–protein interactions, Curr. Protein Pept. Sci. 10 (2009) 196–215.
[9] D.S. Libich, M.A.M. Ahmed, L. Zhong, V.V. Bamm, V. Ladizhansky, G. Harauz, Fuzzy complexes of myelin basic protein—NMR spectroscopic investigations of a polymorphic organizational linker of the central nervous system, Biochem. Cell. Biol. (Special Issue on Protein Folding: Principles and Diseases) 88 (2010) 143–155.
[10] J.N. Whitaker, M.A. Moscarello, P.K. Herman, R.M. Epand, W.K. Surewicz, Conformational correlates of the epitopes of human myelin basic protein peptide 80–89, J. Neurochem. 55 (1990) 568–576.
[11] I.R. Bates, J.M. Boggs, J.B. Feix, G. Harauz, Membrane-anchoring and charge effects in the interaction of myelin basic protein with lipid bilayers studied by site-directed spin labeling, J. Biol. Chem. 278 (2003) 29041–29047.
[12] I.R. Bates, J.B. Feix, J.M. Boggs, G. Harauz, An immunodominant epitope of myelin basic protein is an amphipathic alpha-helix, J. Biol. Chem. 279 (2004) 5757–5764.
[13] C. Farès, D.S. Libich, G. Harauz, Solution NMR structure of an immunodominant epitope of myelin basic protein. Conformational dependence on environment of an intrinsically unstructured protein, FEBS J. 273 (2006) 601–614.
[14] A.A. Musse, J.M. Boggs, G. Harauz, Deimination of membrane-bound myelin basic protein in multiple sclerosis exposes an immunodominant epitope, Proc. Natl Acad. Sci. USA 103 (2006) 4422–4427.
[15] J.M. Boggs, I.R. Bates, A.A. Musse, G. Harauz, Interactions of the 18.5 KDa myelin basic protein with lipid bilayers: studies by electron paramagnetic resonance spectroscopy and implications for generation of autoimmunity in multiple sclerosis, in: J.M. Boggs (Ed.), Myelin Basic Protein, Nova Science Publishers, New York, Intrinsically Disordered Proteins, 2008, pp. 105–125.
[16] M.A.M. Ahmed, V.V. Bamm, G. Harauz, V. Ladizhansky, Solid-state NMR spectroscopy of membrane-reconstituted myelin basic protein—conformation and dynamics of an immunodominant epitope, Biophys. J. 99 (2010) 1247–1255.
[17] E. Polverini, G. Rangaraj, D.S. Libich, J.M. Boggs, G. Harauz, Binding of the proline-rich segment of myelin basic protein to SH3-domains—spectroscopic, microarray, and modelling studies of ligand conformation and effects of post-translational modifications, Biochemistry 47 (2008) 267–282.
[18] L. Homchaudhuri, E. Polverini, W. Gao, G. Harauz, J.M. Boggs, Influence of membrane surface charge and post-translational modifications to myelin basic protein on its ability to tether the Fyn-SH3 domain to a membrane in vitro, Biochemistry 48 (2009) 2385–2393.
[19] D.S. Libich, G. Harauz, Solution NMR and CD spectroscopy of an intrinsically disordered, peripheral membrane protein: evaluation of aqueous and membrane-mimetic solvent conditions for studying the conformational adaptability of the 18.5 kDa isoform of myelin basic protein (MBP), Eur. Biophys. J. 37 (2008) 1015–1029.
[20] L. Zhong, V.V. Bamm, M.A. Ahmed, G. Harauz, V. Ladizhansky, Solid-state NMR spectroscopy of 18.5 kDa myelin basic protein reconstituted with lipid vesicles: spectroscopic characterisation and spectral assignments of solvent-exposed protein fragments, Biochim. Biophys. Acta (Biomembranes) 1768 (2007) 3193–3205.
[21] E. Polverini, Molecular modelling of the interaction of myelin basic protein peptides with signalling proteins and effects of post-translational modifications, in: J.M. Boggs (Ed.), Myelin Basic Protein, Nova Science Publishers, New York, Intrinsically Disordered Proteins, 2008, pp. 169–195.
[22] K. Bessonov, V.V. Bamm, G. Harauz, Misincorporation of the proline homologue Aze (azetidine-2-carboxylic acid) into recombinant myelin basic protein, Phytochemistry 71 (2010) 502–507.
[23] P.E. Fraser, C.M. Deber, Structure and function of the proline-rich region of myelin basic protein, Biochemistry 24 (1985) 4593–4598.

[24] A. Rath, A.R. Davidson, C.M. Deber, The structure of "unstructured" regions in peptides and proteins: role of the polyproline II helix in protein folding and recognition, Biopolymers 80 (2005) 179–185.
[25] D. Van Der Spoel, E. Lindahl, B. Hess, G. Groenhof, A.E. Mark, H.J. Berendsen, GROMACS: fast, flexible, and free, J. Comput. Chem. 26 (2005) 1701–1718.
[26] C. Oostenbrink, A. Villa, A.E. Mark, W.F. van Gunsteren, A biomolecular force field based on the free enthalpy of hydration and solvation: the GROMOS force-field parameter sets 53A5 and 53A6, J. Comput. Chem. 25 (2004) 1656–1676.
[27] G. Bussi, D. Donadio, M. Parrinello, Canonical sampling through velocity rescaling, Journal of Chemical Physics 126 (2007), 014101-1-014101-7.
[28] H.J.C. Berendsen, J.P.M. Postma, W.F. Vangunsteren, A. Dinola, J.R. Haak, Molecular dynamics with coupling to an external bath, J. Chem. Phys. 81 (1984) 3684–3690.
[29] W. Humphrey, A. Dalke, K. Schulten, VMD: visual molecular dynamics, J. Mol. Graph. 14 (1996) 33–38.
[30] D. Walther, WebMol—a Java-based PDB viewer, Trends Biochem. Sci. 22 (1997) 274–275.
[31] E.D. Mantzourani, K. Blokar, T.V. Tselios, J.M. Matsoukas, J.A. Platts, T.M. Mavromoustakos, S.G. Grdadolnik, A combined NMR and molecular dynamics simulation study to determine the conformational properties of agonists and antagonists against experimental autoimmune encephalomyelitis, Bioorg. Med. Chem. 16 (2008) 2171–2182.
[32] D.S. Libich, G. Harauz, Backbone dynamics of the 18.5 kDa isoform of myelin basic protein reveals transient α-helices and a calmodulin-binding site, Biophys. J. 94 (2008) 4847–4866.
[33] P. Schulz, T.F. Cruz, M.A. Moscarello, Endogenous phosphorylation of basic protein in myelin of varying degrees of compaction, Biochemistry 27 (1988) 7793–7799.
[34] J.J. Ramwani, R.M. Epand, M.A. Moscarello, Secondary structure of charge isomers of myelin basic protein before and after phosphorylation, Biochemistry 28 (1989) 6538–6543.
[35] G.E. Deibler, A.L. Stone, M.W. Kies, Role of phosphorylation in conformational adaptability of bovine myelin basic protein, Proteins 7 (1990) 32–40.
[36] J. Ramwani, M.A. Moscarello, Phosphorylation of charge isomers (components) of human myelin basic protein: identification of phosphorylated sites, J. Neurochem. 55 (1990) 1703–1710.
[37] E. Polverini, S. Arisi, P. Cavatorta, T. Berzina, L. Cristofolini, A. Fasano, P. Riccio, M.P. Fontana, Interaction of myelin basic protein with phospholipid monolayers: mechanism of protein penetration, Langmuir 19 (2003) 872–877.
[38] J.M. Boggs, M.A. Moscarello, D. Papahadjopoulos, Structural organization of myelin: role of lipid–protein interactions determined in model systems, in: P.C. Jost, O.H. Griffith (Eds.), Lipid–Protein Interactions, vol. 2, Wiley-Interscience, New York, 1982, pp. 1–51.
[39] P. Tompa, C. Szasz, L. Buday, Structural disorder throws new light on moonlighting, Trends Biochem. Sci. 30 (2005) 484–489.
[40] H. Inouye, D.A. Kirschner, Membrane interactions in nerve myelin: II. Determination of surface charge from biochemical data, Biophys. J. 53 (1988) 247–260.
[41] T. Mittag, L.E. Kay, J.D. Forman-Kay, Protein dynamics and conformational disorder in molecular recognition, J. Mol. Recognit. 23 (2009) 105–116.
[42] C.M. Atkins, M. Yon, N.P. Groome, J.D. Sweatt, Regulation of myelin basic protein phosphorylation by mitogen-activated protein kinase during increased action potential firing in the hippocampus, J. Neurochem. 73 (1999) 1090–1097.
[43] L.S. DeBruin, J.D. Haines, L.A. Wellhauser, G. Radeva, V. Schonmann, D. Bienzle, G. Harauz, Developmental partitioning of myelin basic protein into membrane microdomains, J. Neurosci. Res. 80 (2005) 211–225.
[44] L.S. DeBruin, J.D. Haines, D. Bienzle, G. Harauz, Partitioning of myelin basic protein into membrane microdomains in a spontaneously demyelinating mouse model for multiple sclerosis, Biochem. Cell Biol. 84 (2006) 993–1005.
[45] L.S. DeBruin, G. Harauz, White matter rafting—membrane microdomains in myelin, Neurochem. Res. 32 (2007) 213–228.
[46] L. Otte, U. Wiedemann, B. Schlegel, J.R. Pires, M. Beyermann, P. Schmieder, G. Krause, R. Volkmer-Engert, J. Schneider-Mergener, H. Oschkinat, WW domain sequence activity relationships identified using ligand recognition propensities of 42 WW domains, Protein Sci. 12 (2003) 491–500.
[47] C.D. Andrew, J. Warwicker, G.R. Jones, A.J. Doig, Effect of phosphorylation on alpha-helix stability as a function of position, Biochemistry 41 (2002) 1897–1905.
[48] A.A. Bielska, N.J. Zondlo, Hyperphosphorylation of tau induces local polyproline II helix, Biochemistry 45 (2006) 5527–5537.
[49] R.E. Martenson, M.J. Law, G.E. Deibler, Identification of multiple in vivo phosphorylation sites in rabbit myelin basic protein, J. Biol. Chem. 258 (1983) 930–937.
[50] G.L. Stoner, Predicted folding of beta-structure in myelin basic protein, J. Neurochem. 43 (1984) 433–447.
[51] G.L. Stoner, Conservation throughout vertebrate evolution of the predicted beta-strands in myelin basic protein, J. Neurochem. 55 (1990) 1404–1411.
[52] D.R. Beniac, M.D. Luckevich, G.J. Czarnota, T.A. Tompkins, R.A. Ridsdale, F.P. Ottensmeyer, M.A. Moscarello, G. Harauz, Three-dimensional structure of myelin basic protein. I. Reconstruction via angular reconstitution of randomly oriented single particles, J. Biol. Chem. 272 (1997) 4261–4268.
[53] R.A. Ridsdale, D.R. Beniac, T.A. Tompkins, M.A. Moscarello, G. Harauz, Three-dimensional structure of myelin basic protein. II. Molecular modeling and considerations of predicted structures in multiple sclerosis, J. Biol. Chem. 272 (1997) 4269–4275.
[54] D.R. Beniac, D.D. Wood, N. Palaniyar, F.P. Ottensmeyer, M.A. Moscarello, G. Harauz, Cryoelectron microscopy of protein–lipid complexes of human myelin basic protein charge isomers differing in degree of citrullination, J. Struct. Biol. 129 (2000) 80–95.
[55] E. Polverini, A. Fasano, F. Zito, P. Riccio, P. Cavatorta, Conformation of bovine myelin basic protein purified with bound lipids, Eur. Biophys. J. 28 (1999) 351–355.
[56] G.E. Deibler, T.V. Burlin, A.L. Stone, Three isoforms of human myelin basic protein: purification and structure, J. Neurosci. Res. 41 (1995) 819–827.
[57] V. Csizmok, M. Bokor, P. Banki, E. Klement, K.F. Medzihradszky, P. Friedrich, K. Tompa, P. Tompa, Primary contact sites in intrinsically unstructured proteins: the case of calpastatin and microtubule-associated protein 2, Biochemistry 44 (2005) 3955–3964.
[58] E. Nygaard, G.L. Mendz, W.J. Moore, R.E. Martenson, NMR of a peptic peptide spanning the triprolyl sequence in myelin basic protein, Biochemistry 23 (1984) 4003–4010.
[59] A. Tholey, A. Lindemann, V. Kinzel, J. Reed, Direct effects of phosphorylation on the preferred backbone conformation of peptides: a nuclear magnetic resonance study, Biophys. J. 76 (1999) 76–87.
[60] J.A. Marsh, J.D. Forman-Kay, Sequence determinants of compaction in intrinsically disordered proteins, Biophys. J. 98 (2010) 2383–2390.
[61] S. Jeganathan, A. Hascher, S. Chinnathambi, J. Biernat, E.M. Mandelkow, E. Mandelkow, Proline-directed pseudo-phosphorylation at AT8 and PHF1 epitopes induces a compaction of the paperclip folding of tau and generates a pathological (MC-1) conformation, J. Biol. Chem. 283 (2008) 32066–32076.
[62] S. Jeganathan, M. von Bergen, H. Brutlach, H.J. Steinhoff, E. Mandelkow, Global hairpin folding of tau in solution, Biochemistry 45 (2006) 2283–2293.
[63] M.D. Mukrasch, P. Markwick, J. Biernat, M. Bergen, P. Bernado, C. Griesinger, E. Mandelkow, M. Zweckstetter, M. Blackledge, Highly populated turn conformations in natively unfolded tau protein identified from residual dipolar couplings and molecular simulation, J. Am. Chem. Soc. 129 (2007) 5235–5243.
[64] M.D. Mukrasch, S. Bibow, J. Korukottu, S. Jeganathan, J. Biernat, C. Griesinger, E. Mandelkow, M. Zweckstetter, Structural polymorphism of 441-residue tau at single residue resolution, PLoS Biol. 7 (2009) e34.
[65] R.W. Bailey, A.K. Dunker, C.J. Brown, E.C. Garner, M.D. Griswold, Clusterin, a binding protein with a molten globule-like region, Biochemistry 40 (2001) 11828–11840.
[66] M.B. Feinstein, H. Felsenfeld, Reactions of fluorescent probes with normal and chemically modified myelin basic protein and proteolipid. Comparisons with myelin, Biochemistry 14 (1975) 3049–3056.
[67] D. Matulis, C.G. Baumann, V.A. Bloomfield, R.E. Lovrien, 1-anilino-8-naphthalene sulfonate as a protein conformational tightening agent, Biopolymers 49 (1999) 451–458.
[68] G.V. Semisotnov, N.A. Rodionova, O.I. Razgulyaev, V.N. Uversky, A.F. Gripas', R.I. Gilmanshin, Study of the "molten globule" intermediate state in protein folding by a hydrophobic fluorescent probe, Biopolymers 31 (1991) 119–128.
[69] M.W. Nowak, H.A. Berman, Fluorescence studies on the interactions of myelin basic protein in electrolyte solutions, Biochemistry 30 (1991) 7642–7651.
[70] D.S. Libich, G. Harauz, Interactions of the 18.5 kDa isoform of myelin basic protein with Ca2+-calmodulin: in vitro studies using fluorescence microscopy and spectroscopy, Biochem. Cell Biol. 80 (2002) 395–406.
[71] D.S. Libich, C.M.D. Hill, I.R. Bates, F.R. Hallett, S. Armstrong, A. Siemiarczuk, G. Harauz, Interaction of the 18.5-kD isoform of myelin basic protein with Ca2+-calmodulin: effects of deimination assessed by intrinsic Trp fluorescence spectroscopy, dynamic light scattering, and circular dichroism, Protein Sci. 12 (2003) 1507–1521.
[72] P.L. Clark, Z.P. Liu, J. Zhang, L.M. Gierasch, Intrinsic tryptophans of CRABPI as probes of structure and folding, Protein Sci. 5 (1996) 1108–1117.
[73] G.S.T. Smith, L. Chen, V.V. Bamm, J.R. Dutcher, G. Harauz, The interaction of zinc with membrane-associated 18.5 kDa myelin basic protein: an attenuated total reflectance-Fourier transform infrared spectroscopic study, Amino Acids 39 (2010) 739–750.
[74] C. Baran, G.S. Smith, V.V. Bamm, G. Harauz, J.S. Lee, Divalent cations induce a compaction of intrinsically disordered myelin basic protein, Biochem. Biophys. Res. Commun. 391 (2010) 224–229.
[75] L. Homchaudhuri, A.M. De, S.B. Nilsson, K. Bessonov, G.S. Smith, V.V. Bamm, A.A. Musse, G. Harauz, J.M. Boggs, Secondary structure and solvent accessibility of a calmodulin-binding C-terminal segment of membrane-associated myelin basic protein, Biochemistry 49 (2010) 8955–8966.
[76] V.V. Bamm, M.A. Ahmed, G. Harauz, Interaction of myelin basic protein with actin in the presence of dodecylphosphocholine micelles, Biochemistry 49 (2010) 6903–6915.